PLOS ONE

RESEARCH ARTICLE

Expression and purification of a functional heteromeric $GABA_A$ receptor for structural studies

Derek P. Claxton[1¤], **Eric Gouaux**[1,2]*

1 Vollum Institute, Oregon Health and Science University, Portland, Oregon, United States of America, **2** Howard Hughes Medical Institute, Oregon Health and Science University, Portland, Oregon, United States of America

¤ Current address: Department of Molecular Physiology and Biophysics, Vanderbilt University, Nashville, Tennessee, United States of America
* gouauxe@ohsu.edu

Citation: Claxton DP, Gouaux E (2018) Expression and purification of a functional heteromeric $GABA_A$ receptor for structural studies. PLoS ONE 13(7): e0201210. https://doi.org/10.1371/journal.pone.0201210

Editor: Uwe Rudolph, McLean Hospital/ Harvard Medical School, UNITED STATES

Received: May 3, 2018

Accepted: July 10, 2018

Published: July 20, 2018

Data Availability Statement: All relevant data are within the paper and its Supporting Information files.

Funding: This work was supported by an NIH grant from the National Institute of General Medical Sciences (R01-GM100400) to E.G., who is also an Investigator with the Howard Hughes Medical Institute, and by an NRSA postdoctoral fellowship from the National Institute of General Medical Sciences (F32-GM100584) to D.P.C. The funders had no role in study design, data collection and

Abstract

The GABA-gated chloride channels of the Cys-loop receptor family, known as $GABA_A$ receptors, function as the primary gatekeepers of fast inhibitory neurotransmission in the central nervous system. Formed by the pentameric arrangement of five identical or homologous subunits, $GABA_A$ receptor subtypes are defined by the subunit composition that shape ion channel properties. An understanding of the structural basis of distinct receptor properties has been hindered by the absence of high resolution structural information for heteromeric assemblies. Robust heterologous expression and purification protocols of high expressing receptor constructs are vital for structural studies. Here, we describe a unique approach to screen for well-behaving and functional $GABA_A$ receptor subunit assemblies by using the *Xenopus* oocyte as an expression host in combination with fluorescence detection size exclusion chromatography (FSEC). To detect receptor expression, GFP fusions were introduced into the α1 subunit isoform. In contrast to expression of α1 alone, co-expression with the β subunit promoted formation of monodisperse assemblies. Mutagenesis experiments suggest that the α and β subunits can tolerate large truncations in the non-conserved M3/M4 cytoplasmic loop without compromising oligomeric assembly or GABA-gated channel activity, although removal of N-linked glycosylation sites is negatively correlated with expression level. Additionally, we report methods to improve $GABA_A$ receptor expression in mammalian cell culture that employ recombinant baculovirus transduction. From these methods we have identified a well-behaving minimal functional construct for the α1/β1 $GABA_A$ receptor subtype that can be purified in milligram quantities while retaining high affinity agonist binding activity.

Introduction

The magnitude and duration of excitatory signaling events in the central nervous system is controlled by inhibitory neurotransmission mediated primarily by the opening of pentameric

analysis, decision to publish, or preparation of the manuscript.

Competing interests: The authors have declared that no competing interests exist.

ligand-gated ion channels of the Cys-loop receptor family. GABA (γ-aminobutyric acid) functions as the primary inhibitory chemical messenger and elicits membrane hyperpolarization through rapid diffusion of chloride on the millisecond timescale upon binding to cognate $GABA_A$ receptors [1, 2]. These ion channels are also the targets of endogenous neurosteroids [3, 4] and pharmacological compounds that possess sedative and calming properties through receptor modulation, which defines the clinical basis of general anesthetics and anxiolytics [5–7]. The critical role of these receptors in suppressing excitatory inputs is emphasized further by the strong correlation between reduced $GABA_A$ receptor activity and seizure disorders that vary in severity, including the most debilitating epileptic encephalopathies [8–10].

The potential to alter channel gating by allosteric modulators suggests that $GABA_A$ receptors are excellent candidates for targeted therapies. As an example, the benzodiazepine drug class has been employed as an important therapy for controlling epilepsy [11], anxiety [12] and sleep disorders [13] by directly potentiating $GABA_A$ receptor activity. However, parallel to the broad therapeutic benefits of benzodiazepines is the presentation of adverse side effects, such as amnesia and addiction [7], as a result of long term use. Importantly, the explicit molecular mechanism of drug modulation on $GABA_A$ receptors is not known, although the serendipitous discovery of benzodiazepines was made more than 50 years ago [14].

The lack of atomic resolution structural models that define ligand binding sites and conformational states contributes to an incomplete understanding of $GABA_A$ receptor structure and function relationships. Presently, structural and functional studies are interpreted from homology models generated from bacterial homologs [15–18] or related Cys-loop receptors, such as the nicotinic acetylcholine receptor [19–21] or the glutamate-gated chloride channel [22–24]. In general, all Cys-loop receptors share a common core architecture defined by association of five homologous subunits arranged about a central ion-conducting pore as observed in structures of channels formed from unitary subunits, or homo-pentamers [23, 25, 26]. Each subunit consists of a large extracellular amino-terminal domain connected to a four-helix bundle transmembrane domain that contributes residues for ion selectivity. The orthosteric binding site is formed at the interface of adjacent subunits in the amino-terminal domain. Coupling between agonist binding and channel gating is facilitated by an interaction network composed of residues in transmembrane and extracellular domain loops, including the characteristic disulfide [27].

Despite these similarities, most $GABA_A$ receptors exist as heteromers of unique subunit combinations with discrete ion channel and pharmacological properties [28]. So far 19 $GABA_A$ receptor subunits have been identified and separated into classes and isoforms depending on the primary sequence: α(1–6), β(1–3), γ(1–3), δ, ε, θ, π and ρ(1–3). Although formation of homo-pentamers has been reported from *in vitro* studies [25], recapitulation of *in vivo* gating and pharmacology requires two or more subunits [29, 30]. Even though random assembly is unlikely [31], the molecular determinants that drive assembly of specific combinations in defined subunit stoichiometries and organization are not entirely known. Assembly signals encoded within the subunit primary sequence may play a role in limiting receptor subtype diversity [32]. Notably, subunit expression patterns suggest that unique properties of specific subunit combinations are fine tuned to regulate either phasic or tonic inhibition [28]. The most widely distributed receptor combination in adult neurons is the α1/β2/γ2 subtype in a predicted 2α:2β:1γ subunit ratio [33–36]. However, receptors composed of only α/β subunits, which form channels that are strongly antagonized by Zn^{2+} [37–40] with a proposed 2α:3β stoichiometry [41], may play a role during embryonic development [42]. Importantly, incorporation of the γ subunit confers sensitivity to benzodiazepines and the derived clinical benefit is tied to the adjacent α subunit isoform [7, 43].

High resolution models of heteromeric assemblies will support efforts to delineate the structural basis of $GABA_A$ receptor properties by providing a framework to interpret a wealth of functional data. Indeed, recent structures of the cation-selective α4β2 nicotinic receptor arranged with two different subunit stoichiometries provide clues toward their distinct ion channel properties [44]. As a prerequisite to these studies, identification of efficient heterologous expression and isolation methodologies are required to generate sufficient quantities of receptor for structural interrogation via X-ray diffraction or single particle cryo-electron microscopy. Development of such methods is not trivial for eukaryotic membrane proteins because functional expression may be dependent on the host system, require co-factors or posttranslational modifications [45, 46]. Here, we outline an approach for identifying and characterizing a well-behaving heteromeric $GABA_A$ receptor composed of α/β subunits. This approach combines the robust translation efficiency of *Xenopus* oocytes for screening subunit constructs with technological advances for large-scale expression in mammalian cell culture using a modified baculovirus delivery system [47]. We show that the α1/β1 receptor can be expressed and purified in milligram quantities while retaining ligand binding activity. These results set the stage for detailed structural investigation of heteromeric $GABA_A$ receptors and provide a foundation for pursuing other multi-subunit Cys-loop receptor assemblies.

Materials and methods

Genes and construct design

Construction of vectors. The full-length rat $GABA_A$ receptor subunit isoforms α1 (GeneID 29705), β2 (GeneID 25451) and γ2S (GeneID 29709) with the native signal sequence were obtained in the pGEM vector as a gift from Dr. David S. Weiss. GluClα (Gene ID 180086) was also inserted into the pGEM vector. This vector contains a T7 RNA polymerase promoter site for *in vitro* RNA transcription. For expression in insect cells, individual subunits with a leading Kozak sequence were cloned into the pFastBac1 vector where expression is driven by the polyhedron (PH) promoter, or into the pFastBac Dual vector in which case a single virus particle contains both α1 (PH promoter) and β2 (p10 promoter) subunit genes. For expression in mammalian cells, all genes were cloned individually into a novel vector, pEG BacMam [47], where expression is controlled by the human cytomegalovirus (CMV) promoter.

Generation of fluorescent protein fusions and mutagenesis. Identification of the signal peptide for each subunit was made using the SignalP 4.1 server [48]. The location of fluorescent protein insertions and sequence deletions in the M3/M4 loop is shown in S1 Fig. In summary, enhanced green fluorescent protein (EGFP) was inserted into GluClα in the M3/M4 loop as described previously [49]. EGFP was ligated to the M3/M4 loop of the α1 subunit between V399 and K400 using an in-frame non-native Asc1 restriction site (GGGCGCGCC), which adds a three residue linker (G-R-A) on each side of the fluorescent protein to the native receptor sequence. Likewise, mKalama was inserted into the β2 subunit M3/M4 loop between H421 and V422 also using an Asc1 restriction site. To screen M3/M4 loop truncations ("LT") in α1, an amino-terminal fluorescent protein fusion of the α1 subunit was made by inserting GFPuv after the signal peptide (between G27 and Q28) with a 24 residue polypeptide linker (S-S-S-N-N-N-N-N-N-N-N-N-L-G-T-S-G-L-V-P-R-G-S) containing a thrombin protease site. The α1-LT construct was generated by replacing M3/M4 cytoplasmic loop residues Y341-P408 with Thr for a final predicted M3/M4 linker of R-G-T. Likewise, β2-LT was generated by replacing R333-I438 with Gly for a final predicted M3/M4 linker of G-G-T. The β1-LT subunit gene (GeneID 25450) was synthesized and cloned into pEG BacMam by Bio Basic Inc with residues K334-K439 replaced with Gly-Thr for a final predicted M3/M4

linker of G–G–T. Incorporation of fluorescent protein fusions and receptor mutations were made using standard PCR procedures and confirmed by DNA sequencing.

Construct screening in oocytes

RNA synthesis. Circular plasmid DNA in the pGEM vector was linearized with NheI restriction endonuclease followed by *in vitro* synthesis of capped mRNA using the mMESSAGE mMACHINE T7 Ultra kit from Ambion. After polyadenylation, mRNA was precipitated with LiCl, washed with 70% ethanol and re-suspended with DEPC-treated water. Concentration of mRNA was determined by absorbance at 260 nm and the quality was judged by gel electrophoresis.

FSEC analysis and microscopy. For FSEC analysis, defolliculated *Xenopus* oocytes (stage V-VI) were injected with 25–50 ng of total mRNA mixed in defined ratios to obtain expression of specific receptor subtypes. Oocytes were incubated at 16–18˚C in ND-96 solution (96 mM NaCl, 2 mM KCl, 1 mM $MgCl_2$, 1.8 mM $CaCl_2$, 5 mM Hepes pH 7.5) supplemented with 250 μg/mL Amikacin for three to five days. Eight to 12 oocytes were mechanically disrupted by vigorous pipetting in 150 μL TBS pH 7.4 (20 mM Tris-HCl, 150 mM NaCl) followed by detergent solubilization with 40 mM n-dodecyl-β-D-maltopyranoside ($C_{12}M$) in the presence of 2 mM PMSF for 45 minutes with gentle mixing in 1.5 mL Eppendorf tubes. The sample was then centrifuged at 86,000 rcf for 40 minutes and 100 μL of the supernatant injected onto a Superose6 10/300 GL column (GE Healthcare) equilibrated in TBS pH 8.0 buffer containing 1 mM $C_{12}M$ and 1 mM EDTA for analysis by fluorescence detection size exclusion chromatography (FSEC) monitoring EGFP fluorescence (excitation 488 nm, emission 510 nm) as previously described [50]. Ferritin (440 kDa) and EGFP (27 kDa) were used as molecular weight standards to assess the oligomeric integrity of detergent-solubilized receptor. To compare FSEC data of distinct receptor constructs and minimize batch variations in oocyte quality, FSEC traces for each set of experiments shown in the figures are acquired from the same batch and number of oocytes injected with normalized amounts of synthetic mRNA as described in the text. Receptor expression to the oocyte surface was observed using a Zeiss LSM710 laser scanning confocal microscope. Resonance energy transfer studies employed a high intensity laser (488 nm) to photobleach EGFP and subsequently monitor mKalama fluorescence from 410–486 nm.

Electrophysiology. For two electrode voltage clamp electrophysiology (TEVC) experiments, 5 ng of total mRNA was injected into defolliculated oocytes. After one to three days incubation at 16–18˚C in ND-96 solution, oocytes were impaled with recording pipettes (0.7–2 MΩ) filled with 3 M KCl. Oocytes were voltage clamped to either -30 mV or -60 mV and perfused with 0.1 or 1 mM GABA in the absence or presence of 10 μM zinc in ND-96 buffer. Analog data were filtered at 50 Hz and digitized at ≥1 kHz. The Axoclamp 2B amplifier (Axon Instruments) and pClamp 10 software (Molecular Devices) were used for data acquisition.

Insect and mammalian cell expression

Recombinant baculovirus production. Baculovirus was generated as described previously [47, 51, 52]. Briefly, subunit constructs harboring a C-terminal His_8 tag in pFastBac1, pFastBac Dual or pEG BacMam vectors were transformed into DH10Bac competent cells for site-specific transposition of the expression cassette into bacmid. Purified bacmid was transfected into $1x10^6$ cells Sf9 cells (Invitrogen™) in a 35 mm dish cultured in serum free Sf-900 III SFM medium using Cellfectin II reagent and incubated at 27˚C. The medium containing P1 virus was harvested four days later. To generate P2 virus, P1 virus was diluted 1000 fold into Sf9 suspension cells at $1x10^6$ cells/mL density and allowed to incubate with shaking (115

rpm) at 27˚C for four days. Afterwards, the cells were removed by centrifugation and the supernatant, containing P2 virus, was filter sterilized. Viruses were stored at 4˚C in the dark supplemented with 2% FBS. P2 virus titer was determined using the Sf9 Easy Titer cell line and the end-point dilution assay [53] or flow cytometry by using the ViroCyt Virus Counter 2100 [54].

Insect cell expression. P2 virus derived from pFastBac1 or pFastBac Dual constructs was used to infect Sf9 or High Five cells (Invitrogen^{TM}) at a density of 1.5-3x10^6 cells/mL cultured in serum free Sf-900 III SFM or Express Five medium using different absolute and relative multiplicity-of-infection (MOI). Absolute MOI is defined as total virus relative to the total number of cells. Relative MOI is defined by the ratio of subunit viruses added to the cells. For transduction of cells with two viruses harboring individual α and β subunits (pFastBac1 constructs), the absolute MOI = 5 while varying the relative MOI between subunits as noted. An absolute MOI = 2 was used for transduction of virus obtained from pFastBac Dual constructs, which contain both α and β subunits. Infected cells were incubated with shaking (115 rpm) at either 27˚C for the duration of the expression trial, or shifted to 20˚C after an initial 18 hours at 27˚C. Each day for five days, 1 mL of cells were pelleted by centrifugation and frozen at -80˚C. The cells were solubilized in TBS pH 7.4 with detergent supplemented with a protease inhibitor cocktail (5 μg/mL aprotinin, 2 μg/mL leupeptin, 1.5 μg/mL pepstatin A, 0.3 mM PMSF) for FSEC analysis as described for oocytes.

Expression and purification from mammalian cells. Virus transduction in mammalian cells followed the protocol described by Goehring et al [47]. In summary, P2 virus was used to infect HEK293 GnTI$^-$ suspension cells (ATCC) at a density of 1.5-3x10^6 cells/mL (absolute MOI = 1.5 while varying relative MOI between subunits as noted) cultured in Gibco Freestyle 293 Expression medium supplemented with 2% FBS and placed in a humidity- and CO_2-controlled incubator on an orbital shaker (130 rpm). The total volume of virus added was less than 10% of the culture volume in all cases. Optimized expression parameters were determined by FSEC analysis of $C_{12}M$ detergent-solubilized cells from 1mL aliquots 48 hours post infection. For large-scale expression and purification of α1/β1 receptor, infected cells were grown for 12 hours at 37˚C followed by 10 mM sodium butyrate addition and shifting culture temperature to 30˚C. After 60–72 hours post-infection, cultures were harvested by centrifugation and processed by sonication (10 min cycle, 5 sec on/off) while stirring on ice in the presence of protease inhibitor cocktail. After clearing the lysate of cell debris by centrifugation, membranes were isolated by ultracentrifugation at 186,000 rcf for 1.5 hours. The membranes were mechanically homogenized using a Dounce tissue grinder and solubilized with 40 mM $C_{12}M$ in TBS pH 8.0 for 1 hour. Insoluble material was removed by ultracentrifugation at 186,000 rcf for 1 hour and the supernatant mixed with ClonTech Talon Co^{2+} affinity resin for three to four hours at 4˚C. The resin was washed with 30mM imidazole and then eluted with 250 mM imidazole buffer including 1 mM $C_{12}M$ or 0.3 mM lauryl maltose neopentyl glycol (L-MNG) detergent. Fractions containing the receptor were pooled and concentrated using a 100 kDa MWCO filter for size exclusion chromatography (SEC) over a Superose6 10/300 GL column. Receptor purity was assessed by SDS-PAGE and coomassie blue staining using a 12.5% Tris-HCl gel. LC-MS was employed to confirm the identity of subunit bands on the gel. Receptor concentration was determined by absorbance at 280 nm assuming an average $A_{280nm}^{0.1\%}$ determined by the following equation:

$$\frac{\left[\left(2 * \left(\frac{\varepsilon\alpha}{MW\alpha}\right)\right) + \left(3 * \left(\frac{\varepsilon\beta}{MW\beta}\right)\right)\right]}{5}$$

Here we assume a subunit ratio of 2:3, α:β, and theoretical molecular weights (MW) and molar

absorption coefficients (ε) for each mature subunit. Theoretical MW (α1-LT = 43.1 kDa, β1-LT = 41.6 kDa) and ε (α1-LT = 55600 M^{-1} cm^{-1}, β1-LT = 72895 M^{-1} cm^{-1}) was calculated from the primary sequence using the ExPASy SIB Bioinformatics Resource Portal [55].

Radioligand binding to purified α1/β1 receptor

Titration of purified receptor using 500 nM muscimol (10% hot, Perkin Elmer) and 1 mg/mL YSi Copper His tag SPA beads suggested a capacity of 100 nM receptor (~100 pmol) per mg of beads. For saturation binding and competition assays, 5 nM (0.5 pmol) purified receptor was mixed with ^{3}H-muscimol (1:10 dilution with cold muscimol, 2 Ci/mmol specific activity) and 1 mg/mL SPA beads in 20 mM Hepes pH 7.35, 150 mM NaCl, 0.3 mM L-MNG in 100 uL final reaction volume. Muscimol was titrated from 3–400 nM to determine K_D, or held constant at 100 nM to determine $K_{i\ (GABA)}$. Counts were recorded on a MicroBeta TriLux luminescence counter from Perkin Elmer. Specific binding was measured with 1 mM GABA as a cold competitor. Each data point was repeated in triplicate for two separate trials and the standard deviations determined. Muscimol K_D was determined from nonlinear least squares fit of specific binding assuming a single site binding model. B_{max} was used to estimate the total number of ^{3}H-muscimol binding sites assuming that all receptor was bound to the SPA beads. The IC_{50} of GABA was determined from fitting the data points of the competition experiment with the Hill equation, which was then used to determine K_i using the following equation:

$$K_i = IC_{50}/(1 + \frac{[muscimol]}{K_D})$$

All fits were performed with the program Origin (OriginLab Corp).

Results

Screening methodology of Cys-loop receptor subunit constructs

Historically, *Xenopus* oocytes have proven a convenient vehicle for heterologous gene expression to assess exogenous ion channel properties by electrophysiological methods because they possess the machinery for gene expression but have low endogenous receptor activities [56, 57]. We have taken advantage of the robust gene expression in oocytes as a tractable platform for screening DNA constructs of the multi-subunit Cys-loop receptors. For our studies, genes were designed as fusions with GFP variants and delivered into the cytoplasm by microinjecting mature oocytes with up to 50 ng of total capped RNA transcripts synthesized *in vitro*. After three to five days at 16˚C, a small batch of oocytes (8–12) expressing the same construct was solubilized in detergent and injected onto a Superose6 column for analysis by fluorescence detection size exclusion chromatography (FSEC) monitoring GFP fluorescence [50]. Elution profiles were interpreted in terms of absolute fluorescence intensity as reflective of expression level and peak symmetry (monodispersity) as indicative of uniformity in oligomeric assembly.

As a benchmark, oocytes were injected with either 20 ng or 50 ng of RNA encoding the well-behaved α subunit of the glutamate-gated chloride channel (GluClα) from *C. elegans*, a homo-pentameric Cys-loop receptor that was crystallized previously [23]. The GluClα construct was designed as a fusion with EGFP within the large cytoplasmic M3/M4 loop (Fig 1A and S1 Fig), which has been shown to not disrupt channel function [49]. After four days, EGFP fluorescence could be observed at the oocyte surface relative to an uninjected control using a laser scanning confocal microscope, consistent with expression of the receptor (Fig 1B). GluClα-EGFP was extracted from the oocytes with n-dodecyl-β-D-maltopyranoside ($C_{12}M$), a mild detergent used for purification and crystallization of GluClα [23, 58]. FSEC

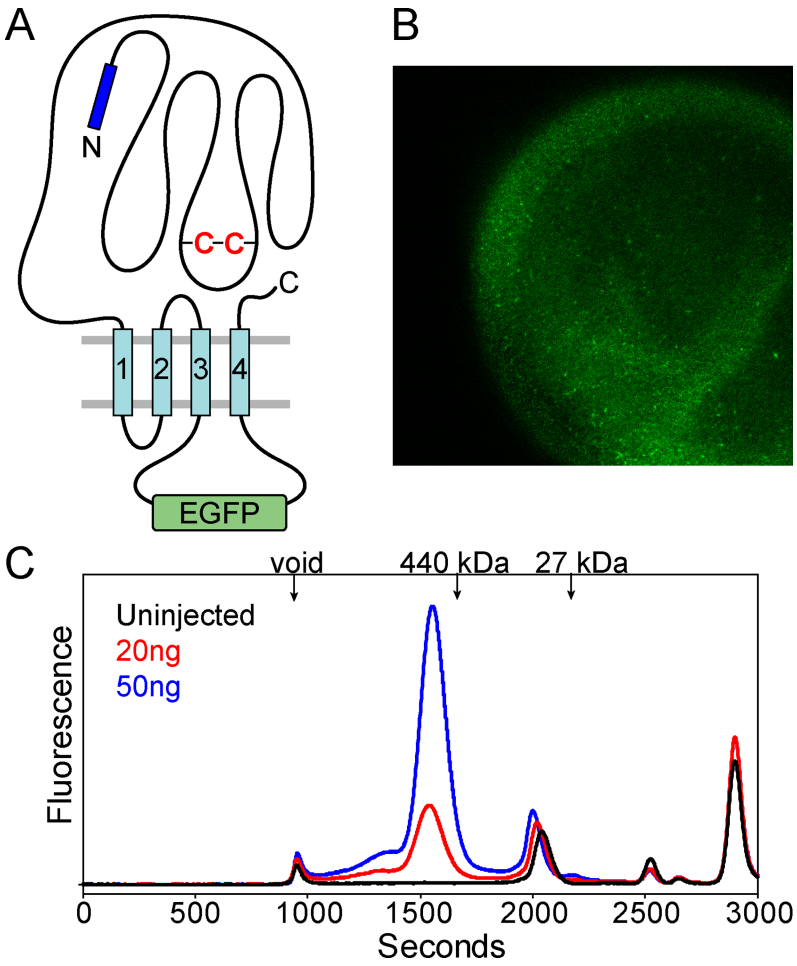

Fig 1. Expression of GluClα-EGFP in oocytes. (A) Cartoon design of EGFP fusion to the M3/M4 loop of GluClα. (B) Four days after injecting 50 ng of synthetic mRNA, receptor expression is visualized by EGFP fluorescence at the oocyte surface by confocal microscopy. (C) Detergent ($C_{12}M$) solubilization of oocytes and FSEC analysis on a Superose6 size exclusion column captures a monodisperse elution profile consistent with a pentameric assembly. Arrows indicate peak elution times for ferritin (440 kDa) and EGFP (27 kDa) standards. Receptor expression levels are sensitive to the total concentration of mRNA injected. FSEC traces were acquired from the same batch of oocytes. Absolute fluorescence intensities are shown.

https://doi.org/10.1371/journal.pone.0201210.g001

analysis detected the receptor peak eluting at a position consistent with an intact detergent-solubilized pentamer (~450 kDa theoretical) based on molecular weight standards (Fig 1C). The GluClα-EGFP elution profile was similar to that observed from detergent-solubilized mammalian cells [47]. The fluorescence intensity of this peak demonstrated sensitivity to the dosage of RNA injected (Fig 1C). Solubilization of uninjected oocytes outlined peaks that are likely to arise from the oocyte itself.

Oocyte expression of $GABA_A$ receptor subunits

The propensity for $GABA_A$ receptor subunits to form homo- or heteromeric channels was investigated by injecting oocytes with the full-length rat α1 isoform as a unitary subunit or in combination with full-length β2 or γ2S subunits, or with all three subunits. Analogous to GluClα in Fig 1A, the α1 subunit was expressed initially as an EGFP fluorescent protein fusion within the non-conserved M3/M4 loop (α1-EGFP), whereas the other subunits were expressed

as wild type sequences. For expression of heteromeric assemblies, synthetic RNA transcripts for each subunit were combined in 1:1 ratios while keeping the total RNA injected constant (25–50 ng).

Three days post-injection, oocytes were solubilized in $C_{12}M$ and analyzed by EGFP fluorescence for expression and profile homogeneity by FSEC. Although the α1 subunit alone demonstrated oligomerization near the elution position of GluClα-EGFP, peak shape is consistent with a heterogeneous entity (Fig 2A). Other peaks in the FSEC trace may suggest the presence of lower order oligomeric species (arrow, Fig 2A). Interestingly, co-injection with the β2 subunit increased overall expression and monodispersity of the primary peak and reduced the population of other oligomeric states, suggesting that incorporation of the β2 subunit coincides with oligomeric stabilization (Fig 2A). In contrast, co-injection with the γ2S (short splice variant) subunit did not alter the heterogeneous profile relative to the α1 subunit alone (Fig 2B), which may indicate that α1/γ2S receptors are unlikely to form stable assemblies in oocytes. However, we know that addition of the γ2S subunit in the presence of α1/β2 enables formation of the most common tri-heteromeric receptor in the central nervous system [34, 35]. Relative to the α1/β2 subunit combination, injection of all three subunits (α1-EGFP/β2/γ2S, 12ng each) resulted in substantially reduced fluorescence intensity (Fig 2C), suggesting either lower expression levels for the tri-heteromeric receptor relative to α1-EGFP/β2 or a reduced number of incorporated α1-EGFP subunits. Given the more robust expression and favorable chromatographic behavior, we continued to pursue characterization of the α1/β2 subtype.

We further investigated the putative association of α1 and β2 subunits by fluorescence resonance energy transfer (FRET) [59] between mKalama, a blue-shifted fluorescent protein, fused to the β2 subunit M3/M4 loop and α1-EGFP using a laser confocal microscope. If FRET occurs, donor (mKalama) fluorescence will be quenched in the presence of the acceptor (EGFP). As shown in Fig 3, photobleaching EGFP at the oocyte surface resulted in an increase in mKalama fluorescence relative to an unbleached control region, suggesting that the fluorescent protein pair is in close enough proximity to undergo FRET and is consistent with the formation of a heteromeric $GABA_A$ receptor composed of α1/β2 subunits.

Based on preliminary screening of a restricted pool of subunits, the α/β $GABA_A$ receptor demonstrated the most promising expression profiles relative to the other tested combinations. To determine a functional α/β construct suitable for large-scale expression, purification and downstream structural studies, we employed systematic mutagenesis to trim potentially unstructured polypeptide regions and remove sites of putative chemical modification in both subunits. The mutagenesis was guided by secondary structure prediction algorithms from the PredictProtein server [60] in conjunction with sequence alignments (S1 Fig) with the homologous GluClα in which a high resolution structure has been solved [23].

M3/M4 loop truncations

The greatest sequence divergence in alignments of $GABA_A$ receptor subunits, and of Cys-loop receptors in general, is found in the large cytoplasmic loop connecting transmembrane helices three and four (M3/M4 loop). Electron microscopy of the related nicotinic acetylcholine receptor has revealed some secondary structure for this loop, but the majority of the peptide chain remains structurally undefined [19]. Although this loop contains a protein-protein interaction motif [61] and charged residues that contribute to the ion permeation pathway [62], agonist activation and ion selectivity persist in Cys-loop receptors when the native loop has been removed [63]. To facilitate crystallization in GluClα, the

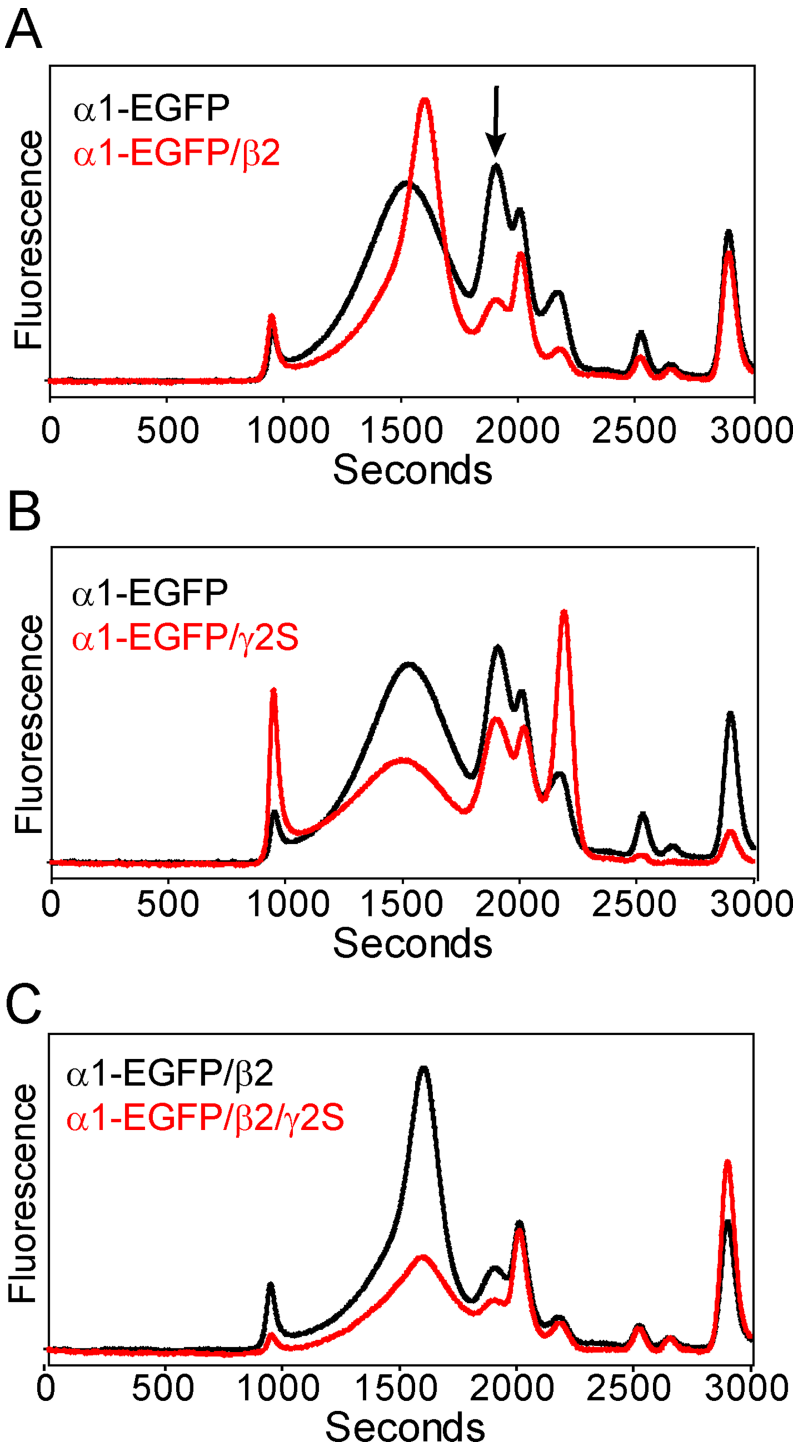

Fig 2. Expression of $GABA_A$ receptors in oocytes. (A) The α1/β2 receptor demonstrates increased expression levels and homogeneity relative to the α1 subunit alone. The arrow indicates a population reduction of smaller oligomers in the presence of the β2 subunit. (B) Co-injection of γ2S mRNA with the α1 subunit does not improve receptor homogeneity. (C) Injection of all three subunits results in attenuated expression levels relative to α1/β2. All FSEC traces were acquired from the same batch of oocytes. Absolute fluorescence intensities are plotted on the same scale.

https://doi.org/10.1371/journal.pone.0201210.g002

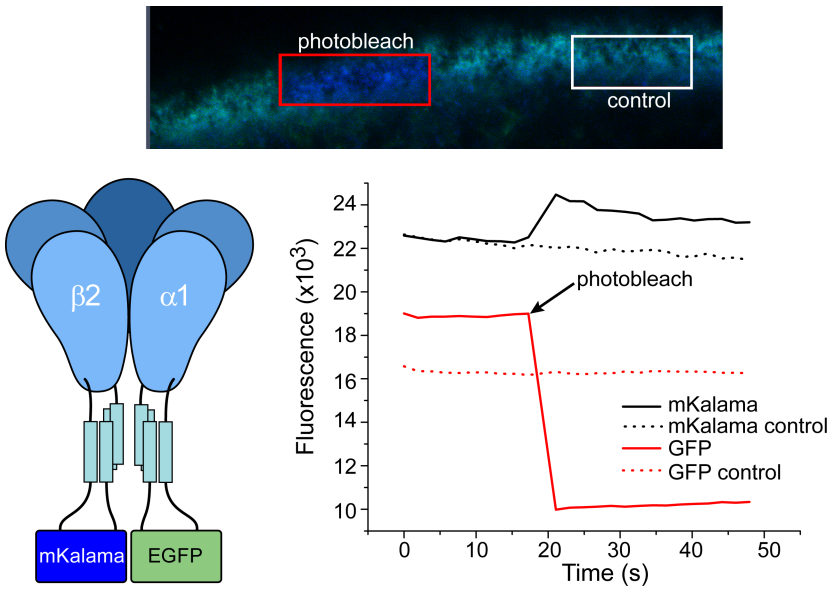

Fig 3. Investigation of α1 and β2 subunit association in oocytes through FRET. Photobleaching of EGFP fused to the α1 subunit results in increased β2-mKalama fluorescence at the oocyte surface relative to a control region, indicating that the subunits are in close enough proximity for subunit fluorescent proteins to undergo FRET.

https://doi.org/10.1371/journal.pone.0201210.g003

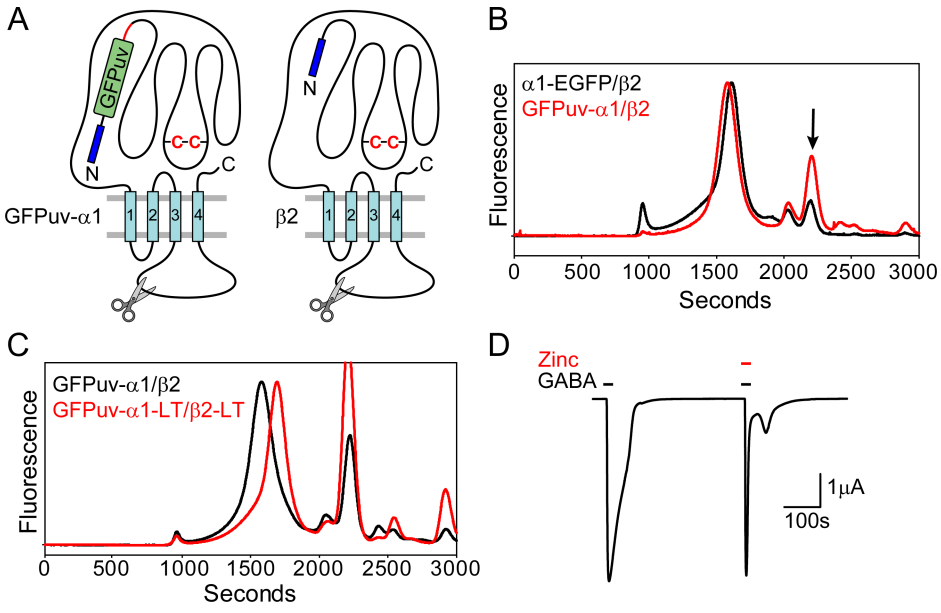

Fig 4. Truncation of the M3/M4 loop does not perturb receptor assembly or function in oocytes. (A) Cartoon of subunit construct design for α1 and β2 subunits shows locations for GFPuv fusion and loop truncation. A polypeptide linker (red line) connects GFPuv to the N-terminus of the α1 subunit. (B) Expression of GFPuv-α1/β2 increases receptor homogeneity relative to α1-EGFP/β2. However, an increase in cleaved GFPuv fluorescence signal is observed (arrow). (C) Replacement of the native M3/M4 loop in both subunits with a tri-peptide induces a right shift in the elution profile, consistent with a smaller hydrodynamic radius. Absolute fluorescence intensities are shown on the same scale. The FSEC traces shown in (B) and (C) were obtained from the same batch of oocytes. (D) Two-electrode voltage clamp of GFPuv-α1-LT/β2-LT demonstrating that the receptor retains gating activity and sensitivity to zinc.

https://doi.org/10.1371/journal.pone.0201210.g004

predicted 58-residue M3/M4 loop was replaced with the tri-peptide linker Ala-Gly-Thr without altering pentamer formation or channel function [23].

In order to screen M3/M4 loop modifications of the α1 subunit, a new fluorescent protein fusion was generated with the cycle 3 GFP variant GFPuv [64] attached to the N-terminus with a 24 amino acid linker following the predicted signal peptide, designated GFPuv-α1 (Fig 4A). Previous work with the nicotinic acetylcholine receptor indicated that N- or C-terminal GFP fusions did not support proper folding of the chromophore, necessitating placement of GFP in the M3/M4 loop [65]. However, GFPuv is more stable [66] and has been used to study the secretory pathway of class C GPCRs [67]. RNA injection of this fusion construct in oocytes and subsequent FSEC analysis indicated that the GFPuv-α1/β2 receptor expressed with reduced aggregation propensity relative to α1-EGFP/β2 (Fig 4B). Of note, this construct demonstrated higher levels of free fluorescent protein following solubilization as indicated by the arrow in Fig 4B, which is likely a consequence of proteolytic cleavage along the polypeptide linker between GFPuv and the α1 N-terminus. Nevertheless, the FSEC profile is consistent with a well-behaved receptor, suggesting that the construct is useful for subsequent mutagenesis.

A large truncation of the M3/M4 loop was designed for both subunits (S1 Fig), reminiscent of the optimized GluClα construct [23], to investigate changes to the receptor elution profile. In the α1 and β2 subunits, the 70- and 108-residue M3/M4 loops were replaced with Arg-Gly-Thr and Gly-Gly-Thr tri-peptide linkers, respectively (defined as "LT" for loop truncation). Combining the loop truncations in both subunits reduced the molecular weight of the receptor by nearly 51 kDa assuming a subunit assembly ratio of 2:3, α1 to β2. This change in mass is reflected in a 100 second right shift in the FSEC elution peak of GFPuv-α1-LT/β2-LT (Fig 4C). We confirmed that this receptor construct retained gating activity by TEVC experiments. A large amplitude current (μA) was elicited from oocyte perfusion with 0.1 mM GABA that was also antagonized by Zn^{2+} (Fig 4D).

N- and C-terminal deletions and removal of glycosylation sites

Construct optimization of GluClα further required deletion of a long stretch of 41 residues in the amino-terminus following the signal peptide and a short carboxy-terminal tail [23] (Fig 5A and 5B). In sequence alignments, the α1 carboxy-terminus extends beyond both GluClα and β2 subunits. The last eleven residues in the α1 subunit were removed by mutagenesis. Oocyte expression of this mutant in the GFPuv-α1-LT/β2-LT context did not perturb receptor assembly (Fig 5C). Both $GABA_A$ receptor α1 and β2 subunits are predicted to have longer signal peptides relative to GluClα, but shorter amino-termini that precede the predicted α-helix in the extracellular domain (Fig 5A). In striking contrast to deletion of the α1 carboxy-terminus, deletion of nine residues from the amino-terminus in the α1-EGFP subunit and seven residues in the full length β2 subunit demonstrated substantially reduced expression levels relative to wild type as indicated by lower absolute fluorescence intensity in the FSEC trace (Fig 5D). Combining the deletion constructs nearly abolished expression of the receptor.

Both subunit amino-terminal deletions contain a consensus site for *N*-linked glycosylation (Asn-X-Ser/Thr), which may play a role in surface expression and function of $GABA_A$ receptors [68, 69]. To test this possibility, each of these sites (α1-N37, β2-N32 in the mature receptor) was mutated to either Asp or Ala in the wild type subunit background and then each subunit was individually examined for changes in receptor expression. As shown in Fig 5E, expression levels were attenuated to similar levels as the amino-terminal deletion constructs with mutation of either Asn residue, although mutation in the β2 subunit was more tolerated.

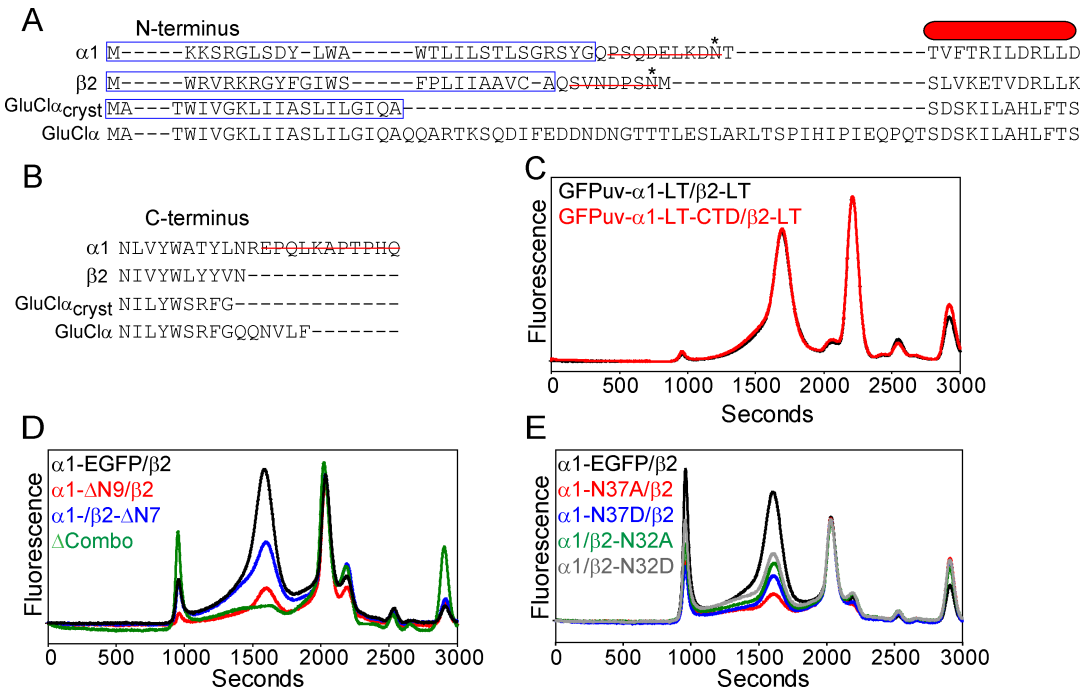

Fig 5. Removal of glycosylation sites on the N-terminus reduces α1/β2 expression in oocytes. (A) Sequence alignment of the N-terminus for $GABA_A$ and GluClα subunits identifying residues for deletion (red line) and predicted sites for glycosylation (*). The red bar represents the first predicted α-helix in the extracellular domain. A blue box outlines the predicted signal peptide. GluClα$_{cryst}$ is the sequence used to obtain the crystal structure. (B) Sequence alignment of the C-terminus for $GABA_A$ and GluClα subunits identifying residues for deletion (red line). (C) Removal of an 11-residue tail from the α1 subunit in the GFPuv-α1-LT/β2-LT construct (Fig 4) does not change receptor behavior. (D) Deletion of the N-terminus (ΔN) in either α1 or β2 subunit reduces receptor expression in the α1-EGFP/β2 construct. (E) Site directed mutagenesis of predicted glycosylation sites reduces α1-EGFP/β2 receptor expression. Absolute fluorescence intensities are shown on the same scale. FSEC traces shown in (D) and (E) were obtained from the same batch of oocytes.

https://doi.org/10.1371/journal.pone.0201210.g005

This result suggested that prevention of post-translational modification with *N*-glycans contributes to diminished expression levels. However, based on these experiments alone, we cannot rule out the potential negative contribution of other deleted residues in the N-terminus to overall expression.

In addition to these sites, the α1 and β2 subunits contain one (N137) and two (N104, N173) other putative glycosylation sites, respectively. The role of post-translational modifications at these sites was investigated using the GFPuv-α1-LT/β2-LT construct. Site directed mutagenesis experiments indicated that mutation of both β2 subunit sites lowered expression levels and increased receptor heterogeneity (Fig 6), suggesting that all three glycosylation sites in the β2 subunit are needed for proper folding and/or targeting. This result is consistent with the observation that mutation of each of the three sites in β2 reduced peak amplitudes and altered gating properties in cultured mammalian cells [69]. Furthermore, all three sites were found to be modified with *N*-glycans in the β3 homo-pentamer [25]. However, mutation of N137 in the α1 subunit does not appear to impede receptor expression in oocytes or substantially change monodispersity, which may indicate that glycosylation at this site is not crucial for α/β receptor assembly. Although previous studies suggested that mutation of N37, N137 or both to Gln in α1 does not impair channel gating in oocytes [68], bulk expression levels appear to be sensitive to the removal of the N37 glycosylation site based on these results. Overall, the data is consistent with the notion that glycosylation plays a crucial role in receptor maturation.

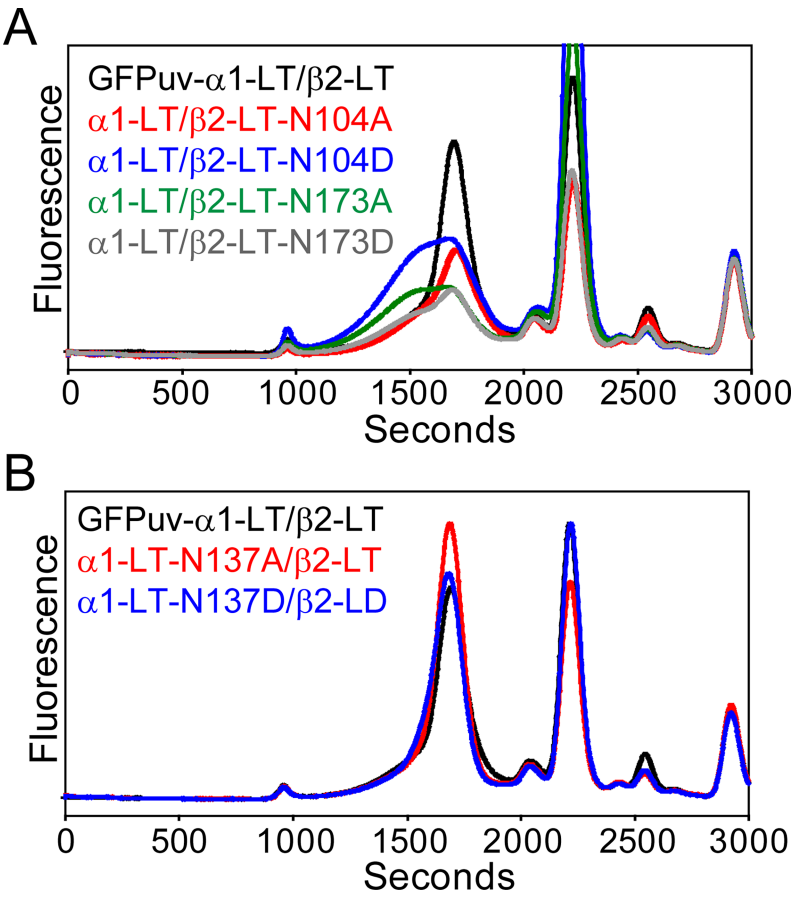

Fig 6. Mutation of other predicted glycosylation sites in the β2 subunit alters receptor expression and assembly in oocytes. (A) Site directed mutation of consensus glycosylation sites in the β2 subunit alters receptor expression and monodispersity, which is in contrast to mutation of a second predicted glycosylation site in the α1subunit (B). Absolute fluorescence intensities are shown on the same scale. FSEC traces were obtained from the same batch of oocytes.

https://doi.org/10.1371/journal.pone.0201210.g006

Expression of the α/β GABA$_A$ receptor in suspension culture

Encouraged by the positive screening results for the rat α1/β2 receptor in oocytes, we investigated suspension cell culture conditions to increase receptor yields for subsequent purification. Preliminary studies were performed in insect cells because homomeric GluClα [23, 58] and heteromeric GABA$_A$ receptors [29, 70] have been expressed previously in Sf9 cells. For these experiments, recombinant baculoviruses were created for the α1-EGFP and β2 (full length) subunits by shuttling the genes into separate pFastBac1 vectors, or combining the subunits into a single bicistronic pFastBac Dual vector (Fig 7A). Visible EGFP expression localized to the membrane was observed as early as one day post infection of Sf9 cells (Fig 7B). However, FSEC analysis indicated that a homogeneous assembly either failed to form or was not maintained after whole-cell solubilization with $C_{12}M$ at all tested time points (Fig 7C and 7D). Although we attempted to modify infection parameters, expression temperature, and detergent solubilization conditions, the α1/β2 subtype could not be isolated from Sf9 or High Five insect cells (S2 Fig).

We reasoned that mammalian cells may provide a more natural and stabilizing environment for heteromeric assemblies leading to successful membrane extraction. Therefore, the full length α1-EGFP and β2 subunits were cloned individually into a modified baculovirus

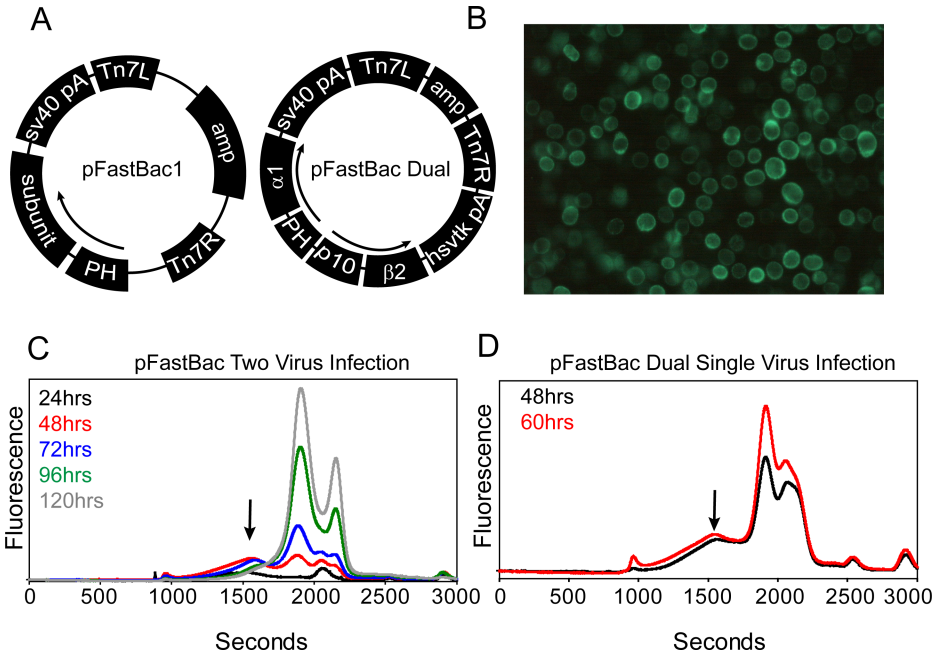

Fig 7. The α1-EGFP/β2 receptor cannot be solubilized by detergent from Sf9 cells. (A) Diagram of insect cell expression vectors harboring one (pFastBac1) or both (pFastBac Dual) full-length GABA$_A$ subunits. EGFP has been placed in the M3/M4 loop of the α1 subunit. (B) EGFP fluorescence is observed 48 hours post infection for pFastBac1 or pFastBac Dual constructs, suggesting receptor targeting to the cell membrane. (C) FSEC analysis at the indicated time points to measure expression suggests that most of the receptor breaks down upon whole cell solubilization with C_{12}M detergent. (D) FSEC profiles do not improve using the bicistronic pFastBac Dual vector, which ensures each cell possesses a copy of both subunits. Absolute fluorescence intensities for (C) and (D) are shown on the same scale.

https://doi.org/10.1371/journal.pone.0201210.g007

vector, pEG BacMam [47], specifically designed to increase protein yields in adherent or suspension mammalian cells (Fig 8A). Efficacious virus was used to co-infect HEK293 suspension cells engineered to be deficient of *N*-acetylglucosaminyltransferase I (GnTI$^-$) and thus eliminate heterogeneous *N*-glycan post-translational modifications [71].

In contrast to insect cells, the α1-EGFP/β2 receptor was observed by FSEC analysis after whole cell solubilization with C_{12}M 48 hours post infection (Fig 8B). Subsequently, expression of the α1-EGFP/β2 receptor was optimized by screening a variety of parameters to improve yields and peak symmetry reported by the FSEC profile. Importantly, several of these parameters were found to be crucial to boosting receptor expression levels and behavior, as illustrated in Fig 8B–8D. First, inclusion of 10 mM sodium butyrate, a histone deacetylase inhibitor, 12 hours post infection increased expression levels ~five-fold relative to virus alone at the cost of increased propensity for receptor aggregation suggested by a strong leading shoulder in the elution peak (Fig 8B). Second, addition of virus with a relative MOI ratio greater than one (β to α) increased receptor monodispersity (Fig 8C). Notably, shifting culture temperature to 30˚C following sodium butyrate supplementation reduced aggregation propensity in addition to a concomitant three-fold increase in fluorescence intensity observed at the 48 hour time point (Fig 8D).

To assess the broad application of these expression conditions, other GABA$_A$ receptor constructs were screened for changes in expression levels in mammalian cells. Indeed, these expression conditions worked well for substantially boosting expression of homomeric (ρ1-EGFP) and mutant heteromeric (α1-EGFP/β2-LT) ion channels (Fig 9A and 9B). Interestingly, exchanging the β2-LT subunit for the β1-LT isoform (similar M3/M4 loop truncation, S1 Fig) further improved receptor homogeneity and enhanced expression by an additional

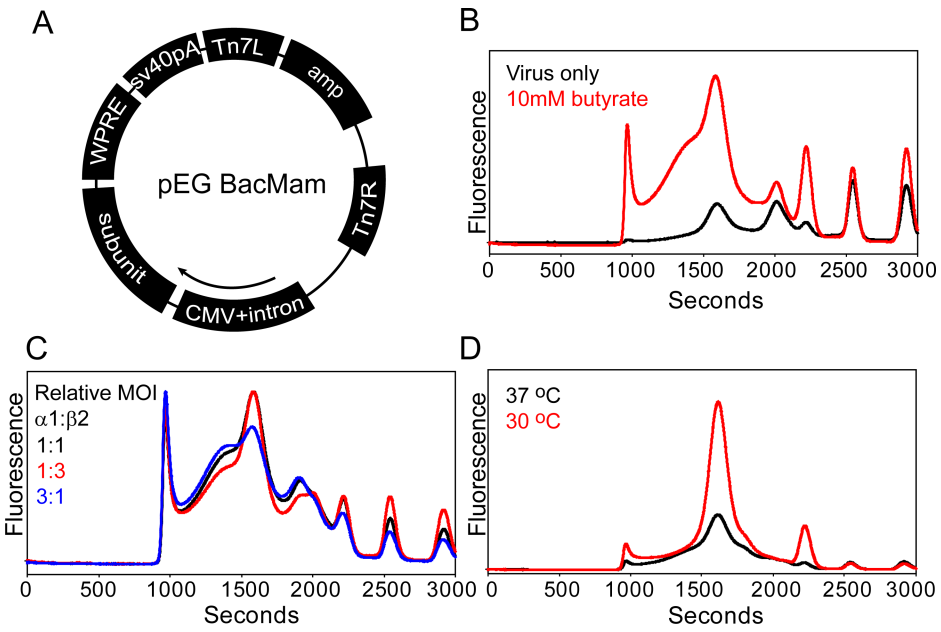

Fig 8. Identification of α1-EGFP/β2 receptor expression parameters in mammalian cells. (A) Diagram of pEG BacMam vector used for generating recombinant baculovirus to infect mammalian cells. (B) Addition of 10 mM sodium butyrate to the virus-transduced culture increases receptor yield but induces aggregation. Absolute fluorescence intensities are shown. (C) Infecting cells with a relative MOI ≥ 1 (β:α) increases receptor monodispersity. Area-normalized traces are shown. Cells were grown at 37˚C for FSEC traces in (B) and (C). (D) Dropping the temperature of infected cells increases receptor yield and reduces aggregation observed at higher temperatures. Absolute fluorescence intensities are shown in (D).

https://doi.org/10.1371/journal.pone.0201210.g008

three fold (Fig 9B). The increased expression levels allowed for an unambiguous evaluation of the importance of the β subunit to formation of monodisperse oligomers in mammalian cells. Consistent with observations made in oocytes, expression of α1-EGFP in the absence of either β1 or β2 yields a polydisperse profile, indicating that assembly of a homogeneous entity requires at least α and β subunits. Additionally, in the presence of either β subunit isoform, introduction of the γ2S subunit to produce tri-heteromeric receptors reduced apparent expression by more than 50% with these methods (S3 Fig). A time course of α1-EGFP/β1-LT receptor expression indicated that the receptor saturated 60–72 hours post infection (Fig 9C). Similar to α1-LT/β2-LT, the α1-LT/β1-LT receptor demonstrated agonist-driven channel activity in oocytes (Fig 9D).

Purification and characterization of the α1/β1 receptor

Based on the expression studies outlined above, we pursued purification of the α1/β1 receptor combination from mammalian cell membranes. Preliminary experiments focused on the α1-EGFP/β1-LT receptor to determine optimal purification strategies (S4 Fig). These experiments suggested that 50–55% of the expressed receptor was isolated from the membrane fraction based on EGFP-FSEC analysis. Subsequently, other receptor constructs containing α1 subunits devoid of EGFP or with truncated M3/M4 loop were isolated and characterized through ligand binding assays. In general, a simple two-step protocol was chosen that combines immobilized metal affinity chromatography (IMAC) followed by gel filtration to remove aggregates and degradation products. An octa-histidine tag was fused to the C-terminus following the thrombin protease recognition sequence in either one or both subunits for IMAC purification and ligand binding analysis via scintillation proximity assay (SPA). Other

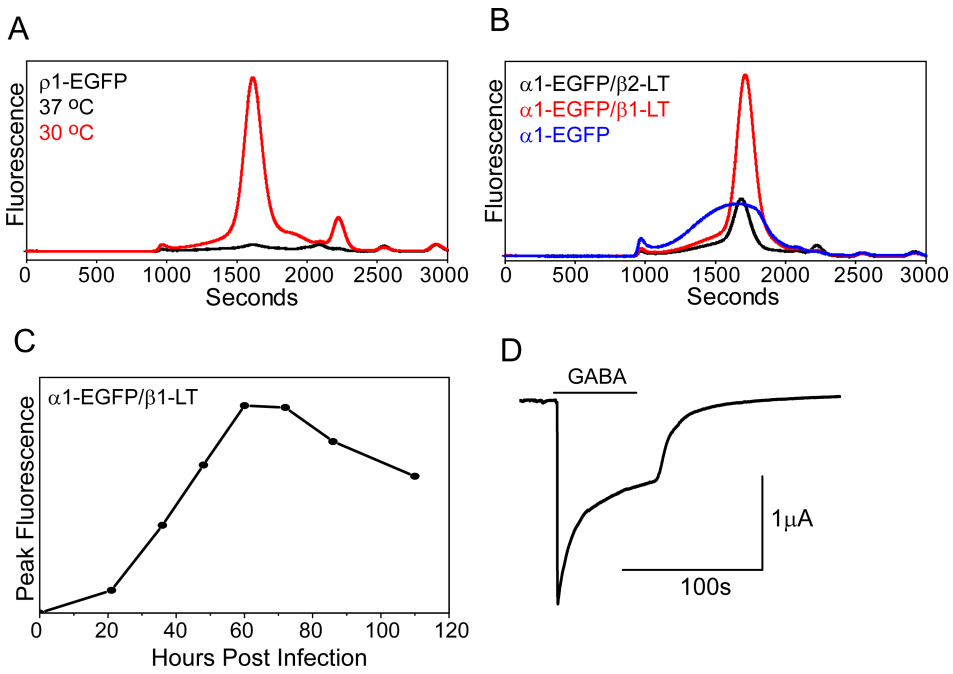

Fig 9. Optimized mammalian expression parameters apply to other receptor GABA$_A$ receptor subtypes. (A) A boost in ρ1-EGFP expression levels is observed at 30˚C with addition of 10 mM sodium butyrate. (B) Similar to oocytes, the β subunit is required to form a homogeneous receptor in mammalian cells. In addition, the α1-EGFP/β1-LT receptor demonstrates higher expression levels than the α1-EGFP/β2-LT receptor. Expression for each experiment was performed at 30˚C. For comparison, the fluorescence scale in (B) is approximately 2-fold greater than in (A). (C) Time course of α1-EGFP/β1-LT expression at 30˚C (relative MOI = 0.6, α1:β1) followed by EGFP-FSEC suggests that the receptor demonstrates peak expression levels 60–72 hours post infection. (D) The α1-LT/β1-LT receptor displays GABA-gated current in oocytes by TEVC measurement.

https://doi.org/10.1371/journal.pone.0201210.g009

elements of primary sequence, such as glycosylation sites, were retained in both subunits to maximize yields.

Following solubilization with 40 mM $C_{12}M$, the α1/β1 receptor was purified successfully into either 1 mM $C_{12}M$ or 0.3 mM lauryl maltose neopentyl glycol (L-MNG) detergent micelles (Fig 10). Typical yields from IMAC purification for all constructs were in the range of 0.4–0.7 mg/L (~2.5 nmol/L) of suspension culture based on absorbance at 280 nm assuming an average $A_{280nm}^{0.1\%}$ (Materials and Methods). Isolation of monodisperse receptor was obtained from preparative size exclusion chromatography (Fig 10A and 10B). SDS-PAGE analysis indicated that the mobility of each subunit corresponds to the expected molecular weight (α1-LT = 43.1 kDa; β1-LT = 41.6 kDa; Fig 10C). Confirmation of the band identities was determined by LC-MS. In addition, each subunit ran as diffuse band(s) that would collapse upon treatment with an endoglycosidase cocktail (S5 Fig), suggesting that the receptor is glycosylated.

The functional integrity of purified receptor was investigated by measuring ^{3}H-muscimol binding activity using SPA. Specific binding of ^{3}H-muscimol was observed in both $C_{12}M$ and L-MNG (Fig 10D). Titration of 0.5 pmol receptor with ^{3}H-muscimol produced a monotonic binding isotherm (Fig 10E). Non-linear least squares fitting assuming a single site binding model revealed a K_D of 24±1.1 nM, consistent with previously reported values for the α1/β1 receptor in intact cells [72]. Assuming that all receptor was bound to the SPA beads, B_{max} corresponded to ~1.5 ^{3}H-muscimol binding sites per receptor. Furthermore, a competition assay in which 100 nM ^{3}H-muscimol was displaced by increasing concentrations of GABA

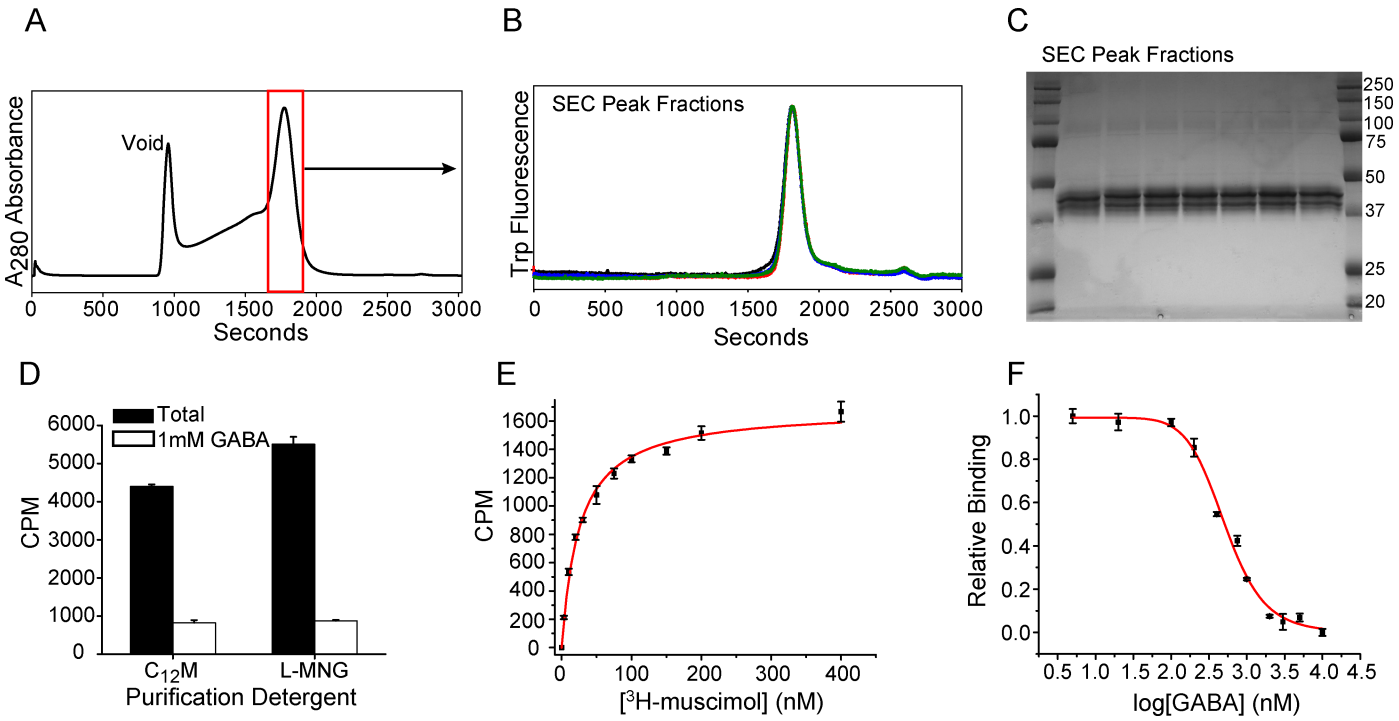

Fig 10. Purification and characterization of the α1/β1 receptor from mammalian cells. (A) Preparative size exclusion chromatography of IMAC-purified material isolates homogeneous receptor as suggested by FSEC analysis of four representative elution fractions collected across the SEC peak (B). (C) SDS-PAGE analysis of SEC fractions across the elution peak shown in (A) indicates diffuse subunit bands, consistent with glycosylation. (D) Purified receptor shows specific binding in $C_{12}M$ or L-MNG detergent. Ligand binding experiments by SPA reveal high affinity binding sites for ^{3}H-muscimol (K_D = 24 nM, B_{max} = 1690 CPM or 0.76 pmol ligand, E) or GABA (K_i = 98 nM, F) as measured by a direct binding isotherm or competition assay, respectively.

https://doi.org/10.1371/journal.pone.0201210.g010

demonstrated an IC_{50} of 507±28 nM and a K_i of 98±6.5 nM (Fig 10F). These results are consistent with the presence of two canonical, high affinity agonist binding sites at the β/α interface [28].

Discussion

Here we have shown that construct screening in *Xenopus* oocytes in combination with FSEC is a viable alternative to previously described approaches, such as *in vitro* transient transfection [50], to identify a suitable heteromeric GABA$_A$ receptor for large-scale expression and purification. This method presents a number of advantages over plasmid DNA transfection, such as straightforward gene delivery, dosage control and ease of manipulation. To enhance plasmid transfection efficiencies, cellular endocytosis is facilitated by cationic "carrier" molecules such as charged lipids or small chemical compounds like calcium phosphate. However, transfection reagents can induce a cytotoxic response and the relative ease of transfection varies with the cell line, which can produce artificially low gene expression levels. Furthermore, protocol optimization becomes more imperative for multi-gene studies, such as with multiple GABA$_A$ receptor subunits, in which overall transfection efficiency becomes compounded. Although viral transduction is an efficient strategy for delivering genetic cargo, making a library of high titer recombinant viruses for expression studies can be time consuming, costly and counter-productive for the iterative pathway of identifying a lead gene construct for expression and downstream structural studies.

Exploiting the GABA$_A$ α1 subunit as a fluorescent protein fusion facilitated rapid construct screening in oocytes by monitoring GFP variant fluorescence as a surrogate reporter of

receptor subtype expression levels and oligomeric integrity [50]. This approach not only led to identification of the α/β subunit combination as a viable candidate for further investigation, but also informed gene design since expression levels and homogeneity were modulated by construct mutagenesis. The application of the FSEC technique for construct screening in oocytes adds a new dimension to the process of identifying the best expressing and behaving constructs. Oocytes provide a tractable platform for identifying functional constructs, but investigating electrophysiological properties alone may lead to false positives since large expression levels are not needed to generate ion channel currents in oocytes. Importantly, the oocyte expression profiles of receptor subtypes investigated here were mirrored by mammalian cells, suggesting continuity between disparate expression systems.

Our approach has underscored important determinants for receptor assembly. Studies have suggested that high affinity binding sites in $GABA_A$ receptors are formed only in the presence of the β subunit [73–75]. As shown in oocytes and mammalian cells, incorporation of the β subunit supports formation of a defined monodisperse assembly consistent with a pentamer. Furthermore, the observation that a monodisperse assembly contains the β subunit was supported by FRET and electrophysiology experiments in oocytes. In the absence of the β subunit, a homogeneous α1 assembly fails to form leading to broad, polydisperse gel filtration profiles that are the hallmark of destabilized oligomers. The lack of a homogeneous receptor population composed of α1 only or α1/γ2S correlates with the lack of functional surface expression previously seen in oocytes [76] or in transfected L929 cells [77]. Our experiments also demonstrate that large truncations in the cytoplasmic M3/M4 loop are not detrimental to expression, subunit association or GABA-gated currents, which is consistent with previous studies of homomeric 5-HT3 and ρ1 receptors [63]. In contrast, interference with subunit glycosylation substantially reduced expression levels.

To our surprise, the most tractable subunit combination identified in oocytes, α1/β2, could not be isolated by detergent from Sf9 or High Five insect cells. A number of studies have shown that di- and tri-heteromeric $GABA_A$ receptors, including α1/β2, can be expressed as functional channels with high affinity ligand binding sites in Sf9 cells using recombinant baculovirus [29, 70, 74]. Notably, these studies examined receptor activity in cell membranes or intact cells. We found that the α1-EGFP/β2 combination expressed to the membrane, which suggested that the receptor is being properly secreted and targeted. However, detergent solubilization resulted in gross breakdown of the receptor as judged by FSEC analysis, which indicated that insect cells are not a practical means of over-expressing and purifying large quantities of intact α1/β2 receptor.

Although the α/β receptor could be expressed in and extracted from mammalian cells, high level expression was only obtained after exploring culture conditions and baculovirus infection parameters. Remarkably, the addition of 10 mM sodium butyrate and the reduction of culture temperature to 30˚C, both of which have been shown to strongly impact protein expression in mammalian cells [51, 78–81], demonstrated a synergistic effect on receptor expression and behavior by increasing the α1/β2 receptor yields approximately 15-fold. Enhancement of protein yields by sodium butyrate has previously been observed to increase rhodopsin 2–3 fold in stable HEK293 cell lines [82], and 10–15 fold in combination with a tetracycline-inducible stable cell line [81].

In addition to culture conditions, co-infection with the β1 subunit drove expression levels even higher than with the β2 subunit. The origin of the difference in expression levels between α1/β1 and α1/β2 subtypes is not clear. Even though the β1 subunit is the most divergent of the three known isoforms, most of the sequence variation in the mature subunit arises from the M3/M4 loop which can be removed without impairing expression or function based on these studies. Furthermore, we note that expression of α/β/γ2S receptors appeared attenuated

relative to α/β in both oocytes and mammalian cells based on a decrease in GFP fluorescence intensity. Since GFP variants have been genetically attached to the α1 subunit, differences in apparent expression levels between α1/β1, α1/β2 and α/β/γ2S receptors may reflect distinct α1 subunit stoichiometries. Alternatively, production of the tri-heteromeric receptor may require an altered expression time course in mammalian cells (Fig 9C). Additionally, lowered expression levels of α/β/γ2S may be a consequence of infection with multiple viruses that is detrimental to cell health. The pliability of pEG BacMam to combine multiple genes into a single vector could be a possible means of increasing α/β/γ2S expression levels by eliminating the need for infecting with multiple viruses.

The purified rat α1/β1 receptor contains high affinity ligand binding sites, consistent with a defined subunit organization that represents native associations. We estimate that 2.5 nmol/L receptor was isolated from the mammalian cell membrane during purification, which corresponds to ~3.8 nmol/L ^{3}H-muscimol sites according to saturation binding analysis (Fig 10). This yield is comparable with that reported for human α1/β3 with an amino-terminal FLAG tag from an HEK293-derived tetracycline-inducable stable cell line (3.2 nmol/L ^{3}H-muscimol sites) [83]. The benefit of the baculovirus system as described here is the ability to rapidly and efficiently express many different constructs without the time consuming process of generating stable cell lines, which is highly advantageous for studies that seek to unveil the role of specific residues in protein structure and function through site directed mutagenesis.

In conclusion, the methods described here have garnered exceptional results toward efficiently expressing and purifying a functional heteromeric $GABA_A$ receptor for structural analysis. Although this approach is focused uniquely upon $GABA_A$ receptors, we anticipate that these methods will be broadly applicable to other complex protein systems that may require multiple protein subunits or binding partners. In general, expression of eukaryotic membrane proteins in our laboratory has benefited immensely using the mammalian system employed here [84–89].

Supporting information

S1 Fig. Sequence alignment and schematic of fluorescent protein fusions and truncations in the M3/M4 loop. Alignment of $GABA_A$ subunit genes used in this study with GluClα highlights regions of sequence variation found in the N-terminus, C-terminus and the M3/M4 loop. The alignment was used in conjunction with the GluClα crystal structure to guide mutagenesis. The alignment was created in CLC Main Workbench 7. Incorporation of an Asc1 restriction site (GRA) was used to insert fluorescent proteins into the M3/M4 loop of either the α1 or β2 subunit. Truncation of the M3/M4 loop of $GABA_A$ subunits were designed to mimic the shortened loop of GluClα (AGT) in the crystal structure. The location of M3 and M4 (red) were derived from alignments with GluClα combined with secondary structure prediction.
(TIF)

S2 Fig. Screening for conditions to express and extract α1-EGFP/β2 from Sf9 or high five insect cells. (A) Infection of Sf9 cells with two baculoviruses harboring the α1-EGFP and β2 subunits at different subunit ratios (relative MOI) does not improve expression as observed 72 hours post infection. (B) Screening a panel of detergents for whole-cell solubilization. (C) Infection of High Five cells or shifting cultures to lower temperatures does not improve receptor recovery. The FSEC traces show absolute fluorescence intensities and are plotted on the same scale as Fig 7C. The arrows point to the expected elution position of the receptor.
(TIF)

S3 Fig. Expression of tri-heteromeric $GABA_A$ receptors in mammalian cells. Incorporation of the γ2S subunit appears to reduce receptor expression levels relative to α1-EGFP/β1-LT (A) or α1-EGFP/β2-LT (B) at similar time points.
(TIF)

S4 Fig. Purification of α1-EGFP/β1-LT from mammalian cells. (A) The receptor demonstrates a similar FSEC profile whether solubilized from whole cells (black trace) or from the membrane fraction (red trace). The traces are normalized to emphasize similarities. Based on the FSEC analysis, approximately 50–55% (~3.3 mg) of the expressed receptor (6.4 L culture) was extracted from the membrane fraction. Of this material, 90% of the receptor was bound to Talon resin after three hours batch binding as reported by a depletion of receptor from the solution (blue trace). Approximately 3mg of receptor (0.5 mg/L or ~2 nmol/L) eluted from the resin (B), and was concentrated for preparative SEC (C). Peak fractions as identified by the red box in (C) are monodisperse by FSEC analysis (D). (E) SDS-PAGE analysis demonstrates the purity of the receptor as a function of purification steps. The first lane shows contaminants eliminated by a wash with 30 mM imidazole during IMAC purification, followed by two lanes showing elution fractions obtained from 250mM imidazole. The following six lanes show purity in fractions obtained across the SEC elution peak, which correspond to the FSEC analysis shown in (D). Notably, the presence of EGFP in the α1 M3/M4 loop enhanced proteolytic cleavage relative to non-fusion constructs, giving rise to a ~30 kDa band in (E). Confirmation that this band contained EGFP was made by in-gel fluorescence prior to fixing and staining (F). Although we did not explicitly determine the identity of this band, the migration position is consistent with EGFP plus the M4 α-helix. However, cleavage of the loop likely does not disrupt native associations since the purified receptor demonstrated monodispersity by FSEC analysis as shown in panel D.
(TIF)

S5 Fig. Endoglycosidase treatment removes N-glycans from α1 and β1 subunits from purified receptor. Following IMAC purification, the receptor was treated with EndoH (1:1, w/w) and $EndoF_3$ (1:50, w/w) for two hours at room temperature at pH 6.5. After purification by SEC, the receptor was analyzed by SDS-PAGE and showed that treatment caused the diffuse bands seen in the IMAC fractions to collapse into a single prominent band for both subunits.
(TIF)

Acknowledgments

The authors wish to thank Dr. David S Weiss of Baylor College of Medicine for providing the α1, β2 and γ2S genes in the pGEM vector. We thank Dr. David C Dawson for providing oocytes and Dr. Haining Zhong for the mKalama fluorescent protein. We also thank Dr. Stefanie Petrie of the OHSU Advanced Light Microscopy Core for expertise and data collection with the Zeiss LSM710 laser scanning confocal microscope. We thank Dr. Richard A Stein of Vanderbilt University for helpful discussions.

Author Contributions

Conceptualization: Eric Gouaux.

Data curation: Derek P. Claxton.

Funding acquisition: Eric Gouaux.

Investigation: Derek P. Claxton.

Methodology: Derek P. Claxton, Eric Gouaux.

Supervision: Eric Gouaux.

Writing – original draft: Derek P. Claxton.

Writing – review & editing: Derek P. Claxton, Eric Gouaux.

References

1. Sigel E, Steinmann ME. Structure, function, and modulation of GABA(A) receptors. J Biol Chem. 2012 Nov 23; 287(48):40224–31. https://doi.org/10.1074/jbc.R112.386664 PMID: 23038269
2. Smart TG, Paoletti P. Synaptic neurotransmitter-gated receptors. Cold Spring Harb Perspect Biol. 2012 Mar; 4(3).
3. Belelli D, Lambert JJ. Neurosteroids: endogenous regulators of the GABA(A) receptor. Nat Rev Neurosci. 2005 Jul; 6(7):565–75. https://doi.org/10.1038/nrn1703 PMID: 15959466
4. Miller PS, Scott S, Masiulis S, De Colibus L, Pardon E, Steyaert J, et al. Structural basis for GABAA receptor potentiation by neurosteroids. Nat Struct Mol Biol. 2017 Nov; 24(11):986–92. https://doi.org/10.1038/nsmb.3484 PMID: 28991263
5. Franks NP. General anaesthesia: from molecular targets to neuronal pathways of sleep and arousal. Nat Rev Neurosci. 2008 May; 9(5):370–86. https://doi.org/10.1038/nrn2372 PMID: 18425091
6. Sieghart W. Structure and pharmacology of gamma-aminobutyric acidA receptor subtypes. Pharmacol Rev. 1995 Jun; 47(2):181–234. PMID: 7568326
7. Tan KR, Rudolph U, Luscher C. Hooked on benzodiazepines: GABA(A) receptor subtypes and addiction. Trends Neurosci. 2011 Feb 24.
8. Allen AS, Berkovic SF, Cossette P, Delanty N, Dlugos D, Eichler EE, et al. De novo mutations in epileptic encephalopathies. Nature. 2013 Aug 11; 501(7466):217–21. https://doi.org/10.1038/nature12439 PMID: 23934111
9. Dibbens LM, Harkin LA, Richards M, Hodgson BL, Clarke AL, Petrou S, et al. The role of neuronal GABA(A) receptor subunit mutations in idiopathic generalized epilepsies. Neurosci Lett. 2009 Apr 10; 453(3):162–5. https://doi.org/10.1016/j.neulet.2009.02.038 PMID: 19429026
10. Macdonald RL, Gallagher MJ, Feng HJ, Kang J. GABA(A) receptor epilepsy mutations. Biochem Pharmacol. 2004 Oct 15; 68(8):1497–506. https://doi.org/10.1016/j.bcp.2004.07.029 PMID: 15451392
11. Riss J, Cloyd J, Gates J, Collins S. Benzodiazepines in epilepsy: pharmacology and pharmacokinetics. Acta Neurol Scand. 2008 Aug; 118(2):69–86. https://doi.org/10.1111/j.1600-0404.2008.01004.x PMID: 18384456
12. Mitte K, Noack P, Steil R, Hautzinger M. A meta-analytic review of the efficacy of drug treatment in generalized anxiety disorder. J Clin Psychopharmacol. 2005 Apr; 25(2):141–50. PMID: 15738745
13. Anderson KN, Shneerson JM. Drug treatment of REM sleep behavior disorder: the use of drug therapies other than clonazepam. J Clin Sleep Med. 2009 Jun 15; 5(3):235–9. PMID: 19960644
14. Ban TA. The role of serendipity in drug discovery. Dialogues Clin Neurosci. 2006; 8(3):335–44. PMID: 17117615
15. Vijayan RS, Trivedi N, Roy SN, Bera I, Manoharan P, Payghan PV, et al. Modeling the closed and open state conformations of the GABA(A) ion channel—plausible structural insights for channel gating. J Chem Inf Model. 2012 Nov 26; 52(11):2958–69. https://doi.org/10.1021/ci300189a PMID: 23116339
16. Hilf RJ, Dutzler R. Structure of a potentially open state of a proton-activated pentameric ligand-gated ion channel. Nature. 2009 Jan 1; 457(7225):115–8. https://doi.org/10.1038/nature07461 PMID: 18987630
17. Hilf RJ, Dutzler R. X-ray structure of a prokaryotic pentameric ligand-gated ion channel. Nature. 2008 Mar 20; 452(7185):375–9. https://doi.org/10.1038/nature06717 PMID: 18322461
18. Bocquet N, Nury H, Baaden M, Le Poupon C, Changeux JP, Delarue M, et al. X-ray structure of a pentameric ligand-gated ion channel in an apparently open conformation. Nature. 2009 Jan 1; 457(7225):111–4. https://doi.org/10.1038/nature07462 PMID: 18987633
19. Unwin N. Refined structure of the nicotinic acetylcholine receptor at 4A resolution. J Mol Biol. 2005 Mar 4; 346(4):967–89. https://doi.org/10.1016/j.jmb.2004.12.031 PMID: 15701510
20. Ernst M, Bruckner S, Boresch S, Sieghart W. Comparative models of GABAA receptor extracellular and transmembrane domains: important insights in pharmacology and function. Mol Pharmacol. 2005 Nov; 68(5):1291–300. https://doi.org/10.1124/mol.105.015982 PMID: 16103045

21. Campagna-Slater V, Weaver DF. Molecular modelling of the GABAA ion channel protein. J Mol Graph Model. 2007 Jan; 25(5):721–30. https://doi.org/10.1016/j.jmgm.2006.06.001 PMID: 16877018

22. Xie HB, Wang J, Sha Y, Cheng MS. Molecular dynamics investigation of Cl(-) transport through the closed and open states of the 2alpha12beta2gamma2 GABA(A) receptor. Biophys Chem. 2013 Oct-Nov; 180–181:1–9. https://doi.org/10.1016/j.bpc.2013.05.004 PMID: 23771165

23. Hibbs RE, Gouaux E. Principles of activation and permeation in an anion-selective Cys-loop receptor. Nature. 2011 Jun 2; 474(7349):54–60. https://doi.org/10.1038/nature10139 PMID: 21572436

24. Puthenkalam R, Hieckel M, Simeone X, Suwattanasophon C, Feldbauer RV, Ecker GF, et al. Structural Studies of GABAA Receptor Binding Sites: Which Experimental Structure Tells us What? Front Mol Neurosci. 2016; 9:44. https://doi.org/10.3389/fnmol.2016.00044 PMID: 27378845

25. Miller PS, Aricescu AR. Crystal structure of a human GABAA receptor. Nature. 2014 Aug 21; 512 (7514):270–5. https://doi.org/10.1038/nature13293 PMID: 24909990

26. Du J, Lu W, Wu S, Cheng Y, Gouaux E. Glycine receptor mechanism elucidated by electron cryo-microscopy. Nature. 2015 Oct 8; 526(7572):224–9. https://doi.org/10.1038/nature14853 PMID: 26344198

27. Cederholm JM, Schofield PR, Lewis TM. Gating mechanisms in Cys-loop receptors. Eur Biophys J. 2009 Dec; 39(1):37–49. https://doi.org/10.1007/s00249-009-0452-y PMID: 19404635

28. Olsen RW, Sieghart W. GABA A receptors: subtypes provide diversity of function and pharmacology. Neuropharmacology. 2009 Jan; 56(1):141–8. https://doi.org/10.1016/j.neuropharm.2008.07.045 PMID: 18760291

29. Pregenzer JF, Im WB, Carter DB, Thomsen DR. Comparison of interactions of [3H]muscimol, t-butylbicyclophosphoro[35S]thionate, and [3H]flunitrazepam with cloned gamma-aminobutyric acidA receptors of the alpha 1 beta 2 and alpha 1 beta 2 gamma 2 subtypes. Mol Pharmacol. 1993 May; 43(5):801–6. PMID: 8388991

30. Pritchett DB, Sontheimer H, Gorman CM, Kettenmann H, Seeburg PH, Schofield PR. Transient expression shows ligand gating and allosteric potentiation of GABAA receptor subunits. Science. 1988 Dec 2; 242(4883):1306–8. PMID: 2848320

31. Connolly CN, Krishek BJ, McDonald BJ, Smart TG, Moss SJ. Assembly and cell surface expression of heteromeric and homomeric gamma-aminobutyric acid type A receptors. J Biol Chem. 1996 Jan 5; 271 (1):89–96. PMID: 8550630

32. Bollan K, King D, Robertson LA, Brown K, Taylor PM, Moss SJ, et al. GABA(A) receptor composition is determined by distinct assembly signals within alpha and beta subunits. J Biol Chem. 2003 Feb 14; 278 (7):4747–55. https://doi.org/10.1074/jbc.M210229200 PMID: 12471031

33. Baumann SW, Baur R, Sigel E. Forced subunit assembly in alpha1beta2gamma2 GABAA receptors. Insight into the absolute arrangement. J Biol Chem. 2002 Nov 29; 277(48):46020–5. https://doi.org/10.1074/jbc.M207663200 PMID: 12324466

34. Chang Y, Wang R, Barot S, Weiss DS. Stoichiometry of a recombinant GABAA receptor. J Neurosci. 1996 Sep 1; 16(17):5415–24. PMID: 8757254

35. Farrar SJ, Whiting PJ, Bonnert TP, McKernan RM. Stoichiometry of a ligand-gated ion channel determined by fluorescence energy transfer. J Biol Chem. 1999 Apr 9; 274(15):10100–4. PMID: 10187791

36. Tretter V, Ehya N, Fuchs K, Sieghart W. Stoichiometry and assembly of a recombinant GABAA receptor subtype. J Neurosci. 1997 Apr 15; 17(8):2728–37. PMID: 9092594

37. Draguhn A, Verdorn TA, Ewert M, Seeburg PH, Sakmann B. Functional and molecular distinction between recombinant rat GABAA receptor subtypes by Zn2+. Neuron. 1990 Dec; 5(6):781–8. PMID: 1702644

38. Hosie AM, Dunne EL, Harvey RJ, Smart TG. Zinc-mediated inhibition of GABA(A) receptors: discrete binding sites underlie subtype specificity. Nat Neurosci. 2003 Apr; 6(4):362–9. https://doi.org/10.1038/nn1030 PMID: 12640458

39. Smart TG, Constanti A. Differential effect of zinc on the vertebrate GABAA-receptor complex. Br J Pharmacol. 1990 Apr; 99(4):643–54. PMID: 2163276

40. Westbrook GL, Mayer ML. Micromolar concentrations of Zn2+ antagonize NMDA and GABA responses of hippocampal neurons. Nature. 1987 Aug 13–19; 328(6131):640–3. https://doi.org/10.1038/328640a0 PMID: 3039375

41. Baumann SW, Baur R, Sigel E. Subunit arrangement of gamma-aminobutyric acid type A receptors. J Biol Chem. 2001 Sep 28; 276(39):36275–80. https://doi.org/10.1074/jbc.M105240200 PMID: 11466317

42. Smart TG, Moss SJ, Xie X, Huganir RL. GABAA receptors are differentially sensitive to zinc: dependence on subunit composition. Br J Pharmacol. 1991 Aug; 103(4):1837–9. PMID: 1655141

43. Pritchett DB, Sontheimer H, Shivers BD, Ymer S, Kettenmann H, Schofield PR, et al. Importance of a novel GABAA receptor subunit for benzodiazepine pharmacology. Nature. 1989 Apr 13; 338 (6216):582–5. https://doi.org/10.1038/338582a0 PMID: 2538761

44. Walsh RM., Roh SH, Gharpure A, Morales-Perez CL, Teng J, Hibbs RE. Structural principles of distinct assemblies of the human alpha4beta2 nicotinic receptor. Nature. 2018 May; 557(7704):261–5. https://doi.org/10.1038/s41586-018-0081-7 PMID: 29720657

45. Baulac S, Huberfeld G, Gourfinkel-An I, Mitropoulou G, Beranger A, Prud'homme JF, et al. First genetic evidence of GABA(A) receptor dysfunction in epilepsy: a mutation in the gamma2-subunit gene. Nat Genet. 2001 May; 28(1):46–8. https://doi.org/10.1038/88254 PMID: 11326274

46. Andrell J, Tate CG. Overexpression of membrane proteins in mammalian cells for structural studies. Mol Membr Biol. 2013 Feb; 30(1):52–63. https://doi.org/10.3109/09687688.2012.703703 PMID: 22963530

47. Goehring A, Lee CH, Wang KH, Michel JC, Claxton DP, Baconguis I, et al. Screening and large-scale expression of membrane proteins in mammalian cells for structural studies. Nat Protoc. 2014 Nov; 9 (11):2574–85. https://doi.org/10.1038/nprot.2014.173 PMID: 25299155

48. Petersen TN, Brunak S, von Heijne G, Nielsen H. SignalP 4.0: discriminating signal peptides from transmembrane regions. Nat Methods. 2011; 8(10):785–6. https://doi.org/10.1038/nmeth.1701 PMID: 21959131

49. Li P, Slimko EM, Lester HA. Selective elimination of glutamate activation and introduction of fluorescent proteins into a Caenorhabditis elegans chloride channel. FEBS Lett. 2002 Sep 25; 528(1–3):77–82. PMID: 12297283

50. Kawate T, Gouaux E. Fluorescence-detection size-exclusion chromatography for precrystallization screening of integral membrane proteins. Structure. 2006 Apr; 14(4):673–81. https://doi.org/10.1016/j.str.2006.01.013 PMID: 16615909

51. Dukkipati A, Park HH, Waghray D, Fischer S, Garcia KC. BacMam system for high-level expression of recombinant soluble and membrane glycoproteins for structural studies. Protein Expr Purif. 2008 Dec; 62(2):160–70. https://doi.org/10.1016/j.pep.2008.08.004 PMID: 18782620

52. Luckow VA. Baculovirus systems for the expression of human gene products. Curr Opin Biotechnol. 1993 Oct; 4(5):564–72. PMID: 7764207

53. Hopkins R, Esposito D. A rapid method for titrating baculovirus stocks using the Sf-9 Easy Titer cell line. Biotechniques. 2009 Sep; 47(3):785–8. https://doi.org/10.2144/000113238 PMID: 19852765

54. Ferris MM, Stepp PC, Ranno KA, Mahmoud W, Ibbitson E, Jarvis J, et al. Evaluation of the Virus Counter(R) for rapid baculovirus quantitation. J Virol Methods. 2011 Jan; 171(1):111–6. https://doi.org/10.1016/j.jviromet.2010.10.010 PMID: 20970458

55. Wilkins MR, Gasteiger E, Bairoch A, Sanchez JC, Williams KL, Appel RD, et al. Protein identification and analysis tools in the ExPASy server. Methods Mol Biol. 1999; 112:531–52. PMID: 10027275

56. Gurdon JB, Lane CD, Woodland HR, Marbaix G. Use of frog eggs and oocytes for the study of messenger RNA and its translation in living cells. Nature. 1971 Sep 17; 233(5316):177–82. PMID: 4939175

57. Weber W. Ion currents of Xenopus laevis oocytes: state of the art. Biochim Biophys Acta. 1999 Oct 15; 1421(2):213–33. PMID: 10518693

58. Althoff T, Hibbs RE, Banerjee S, Gouaux E. X-ray structures of GluCl in apo states reveal a gating mechanism of Cys-loop receptors. Nature. 2014 Aug 21; 512(7514):333–7. https://doi.org/10.1038/nature13669 PMID: 25143115

59. Lakowicz JR. Principles of fluorescence spectroscopy. 3rd ed. New York: Springer; 2006.

60. Rost B, Yachdav G, Liu J. The PredictProtein server. Nucleic Acids Res. 2004 Jul 1; 32(Web Server issue):W321–6. https://doi.org/10.1093/nar/gkh377 PMID: 15215403

61. Chen ZW, Olsen RW. GABAA receptor associated proteins: a key factor regulating GABAA receptor function. J Neurochem. 2007 Jan; 100(2):279–94. https://doi.org/10.1111/j.1471-4159.2006.04206.x PMID: 17083446

62. O'Toole KK, Jenkins A. Discrete M3-M4 intracellular loop subdomains control specific aspects of gamma-aminobutyric acid type A receptor function. J Biol Chem. 2011 Nov 4; 286(44):37990–9. https://doi.org/10.1074/jbc.M111.258012 PMID: 21903587

63. Jansen M, Bali M, Akabas MH. Modular design of Cys-loop ligand-gated ion channels: functional 5-HT3 and GABA rho1 receptors lacking the large cytoplasmic M3M4 loop. J Gen Physiol. 2008 Feb; 131 (2):137–46. https://doi.org/10.1085/jgp.200709896 PMID: 18227272

64. Crameri A, Whitehorn EA, Tate E, Stemmer WP. Improved green fluorescent protein by molecular evolution using DNA shuffling. Nat Biotechnol. 1996 Mar; 14(3):315–9. https://doi.org/10.1038/nbt0396-315 PMID: 9630892

65. Gensler S, Sander A, Korngreen A, Traina G, Giese G, Witzemann V. Assembly and clustering of acetylcholine receptors containing GFP-tagged epsilon or gamma subunits: selective targeting to the neuromuscular junction in vivo. Eur J Biochem. 2001 Apr; 268(8):2209–17. PMID: 11298737

66. Fukuda H, Arai M, Kuwajima K. Folding of green fluorescent protein and the cycle3 mutant. Biochemistry. 2000 Oct 3; 39(39):12025–32. PMID: 11009617

67. Ashikawa Y, Ihara M, Matsuura N, Fukunaga Y, Kusakabe Y, Yamashita A. GFP-based evaluation system of recombinant expression through the secretory pathway in insect cells and its application to the extracellular domains of class C GPCRs. Protein Sci. 2011 Oct; 20(10):1720–34. https://doi.org/10.1002/pro.707 PMID: 21805523

68. Buller AL, Hastings GA, Kirkness EF, Fraser CM. Site-directed mutagenesis of N-linked glycosylation sites on the gamma-aminobutyric acid type A receptor alpha 1 subunit. Mol Pharmacol. 1994 Nov; 46 (5):858–65. PMID: 7969072

69. Lo WY, Lagrange AH, Hernandez CC, Harrison R, Dell A, Haslam SM, et al. Glycosylation of {beta}2 subunits regulates GABAA receptor biogenesis and channel gating. J Biol Chem. 2010 Oct 8; 285 (41):31348–61. https://doi.org/10.1074/jbc.M110.151449 PMID: 20639197

70. Carter DB, Thomsen DR, Im WB, Lennon DJ, Ngo DM, Gale W, et al. Functional expression of GABAA chloride channels and benzodiazepine binding sites in baculovirus infected insect cells. Biotechnology (N Y). 1992 Jun; 10(6):679–81.

71. Reeves PJ, Callewaert N, Contreras R, Khorana HG. Structure and function in rhodopsin: high-level expression of rhodopsin with restricted and homogeneous N-glycosylation by a tetracycline-inducible N-acetylglucosaminyltransferase I-negative HEK293S stable mammalian cell line. Proc Natl Acad Sci U S A. 2002 Oct 15; 99(21):13419–24. https://doi.org/10.1073/pnas.212519299 PMID: 12370423

72. Tierney ML, Birnir B, Pillai NP, Clements JD, Howitt SM, Cox GB, et al. Effects of mutating leucine to threonine in the M2 segment of alpha1 and beta1 subunits of GABAA alpha1beta1 receptors. J Membr Biol. 1996 Nov; 154(1):11–21. PMID: 8881023

73. Amin J, Weiss DS. GABAA receptor needs two homologous domains of the beta-subunit for activation by GABA but not by pentobarbital. Nature. 1993 Dec 9; 366(6455):565–9. https://doi.org/10.1038/366565a0 PMID: 7504783

74. Birnir B, Tierney ML, Howitt SM, Cox GB, Gage PW. A combination of human alpha 1 and beta 1 subunits is required for formation of detectable GABA-activated chloride channels in Sf9 cells. Proc Biol Sci. 1992 Dec 22; 250(1329):307–12. https://doi.org/10.1098/rspb.1992.0163 PMID: 1283641

75. Casalotti SO, Stephenson FA, Barnard EA. Separate subunits for agonist and benzodiazepine binding in the gamma-aminobutyric acidA receptor oligomer. J Biol Chem. 1986 Nov 15; 261(32):15013–6. PMID: 3021761

76. Connor JX, Boileau AJ, Czajkowski C. A GABAA receptor alpha1 subunit tagged with green fluorescent protein requires a beta subunit for functional surface expression. J Biol Chem. 1998 Oct 30; 273 (44):28906–11. PMID: 9786893

77. Angelotti TP, Macdonald RL. Assembly of GABAA receptor subunits: alpha 1 beta 1 and alpha 1 beta 1 gamma 2S subunits produce unique ion channels with dissimilar single-channel properties. J Neurosci. 1993 Apr; 13(4):1429–40. PMID: 7681870

78. Hsu CS, Ho YC, Wang KC, Hu YC. Investigation of optimal transduction conditions for baculovirus-mediated gene delivery into mammalian cells. Biotechnol Bioeng. 2004 Oct 5; 88(1):42–51. https://doi.org/10.1002/bit.20213 PMID: 15384054

79. Wulhfard S, Tissot S, Bouchet S, Cevey J, De Jesus M, Hacker DL, et al. Mild hypothermia improves transient gene expression yields several fold in Chinese hamster ovary cells. Biotechnol Prog. 2008 Mar-Apr; 24(2):458–65. https://doi.org/10.1021/bp070286c PMID: 18220408

80. Palermo DP, DeGraaf ME, Marotti KR, Rehberg E, Post LE. Production of analytical quantities of recombinant proteins in Chinese hamster ovary cells using sodium butyrate to elevate gene expression. J Biotechnol. 1991 Jun; 19(1):35–47. PMID: 1369310

81. Reeves PJ, Kim JM, Khorana HG. Structure and function in rhodopsin: a tetracycline-inducible system in stable mammalian cell lines for high-level expression of opsin mutants. Proc Natl Acad Sci U S A. 2002 Oct 15; 99(21):13413–8. https://doi.org/10.1073/pnas.212519199 PMID: 12370422

82. Reeves PJ, Klein-Seetharaman J, Getmanova EV, Eilers M, Loewen MC, Smith SO, et al. Expression and purification of rhodopsin and its mutants from stable mammalian cell lines: application to NMR studies. Biochem Soc Trans. 1999 Dec; 27(6):950–5. PMID: 10830134

83. Dostalova Z, Liu A, Zhou X, Farmer SL, Krenzel ES, Arevalo E, et al. High-level expression and purification of Cys-loop ligand-gated ion channels in a tetracycline-inducible stable mammalian cell line: GABAA and serotonin receptors. Protein Sci. 2010 Sep; 19(9):1728–38. https://doi.org/10.1002/pro.456 PMID: 20662008

84. Baconguis I, Gouaux E. Structural plasticity and dynamic selectivity of acid-sensing ion channel-spider toxin complexes. Nature. 2012 Sep 20; 489(7416):400–5. https://doi.org/10.1038/nature11375 PMID: 22842900

85. Penmatsa A, Wang KH, Gouaux E. X-ray structure of dopamine transporter elucidates antidepressant mechanism. Nature. 2013 Nov 7; 503(7474):85–90. https://doi.org/10.1038/nature12533 PMID: 24037379

86. Lee CH, Lu W, Michel JC, Goehring A, Du J, Song X, et al. NMDA receptor structures reveal subunit arrangement and pore architecture. Nature. 2014 Jul 10; 511(7508):191–7. https://doi.org/10.1038/nature13548 PMID: 25008524

87. Coleman JA, Green EM, Gouaux E. X-ray structures and mechanism of the human serotonin transporter. Nature. 2016 Apr 21; 532(7599):334–9. https://doi.org/10.1038/nature17629 PMID: 27049939

88. Mansoor SE, Lu W, Oosterheert W, Shekhar M, Tajkhorshid E, Gouaux E. X-ray structures define human P2X(3) receptor gating cycle and antagonist action. Nature. 2016 Oct 6; 538(7623):66–71. https://doi.org/10.1038/nature19367 PMID: 27626375

89. Yoder N, Yoshioka C, Gouaux E. Gating mechanisms of acid-sensing ion channels. Nature. 2018 Mar 15; 555(7696):397–401. https://doi.org/10.1038/nature25782 PMID: 29513651